Soil and Foundation Conditions and Ground Motion at Cypress Street Viaduct

G. NORRIS, R. SIDDHARTHAN, Z. ZAFIR, AND P. GOWDA

The Cypress Street viaduct, located some 100 km (60 mi) from the epicenter of the Loma Prieta, California, earthquake, suffered catastrophic structural damage during the 5 to 10 sec of strong shaking on October 17, 1989. Although much has been written about the structural details that ultimately led to the viaduct's failure, less has been presented relative to the possible contributing effect of the soil and foundations. The results of this study show the difference in the soils and foundations (spread footings and short end bearing piles in Merritt sand, abruptly changing to long friction piles in Bay mud) along the length of the viaduct and the possible difference in ground surface motions over the northern (Bay mud) versus the southern (Merritt sand) sections. Given the soil borings at Bents 61 and 97, the nonlinear variations in both the rotational and lateral pile group stiffnesses are assessed and presented for consideration. The lateral response is compared with the measured response from California Department of Transportation lateral pile group load tests. There is such a difference in the lateral and rotational stiffnesses of pile groups in the Merritt sand versus the Bay mud that, given the abrupt change in soil and foundation conditions between Bents 71 and 72, a dynamic analysis intending to show the progress and arrest of collapse along the length of the viaduct would need to take this into consideration. In regard to the stiffness evaluations, the authors considered the effect of developing porewater pressure in the Merritt sand and the choice of free-field versus near-field (or inertial interaction) strain for the evaluation of soil modulus values for stiffness calculations. The discussion in this paper covers subsurface conditions, site ground motions, the associated collapse, foundation types, soil properties, and porewater pressure buildup in the Merritt sand during the Loma Prieta earthquake.

The collapse of roughly a 1.25-km (¾-mi) length of the northern portion of the Cypress Street viaduct of the Nimitz Freeway (Interstate 880) during the Loma Prieta earthquake of October 17, 1989, claimed 40 lives. This double-decker structure, shown in Figure 1 (*1*), was designed in the early 1950s and built in the late 1950s; it was located some 100 km (60 mi) north of the earthquake epicenter. Figure 2 shows the location of the structure in relation to various areas that experienced liquefaction of the loose hydraulic sand fill employed in their construction (e.g., the Oakland harbor complex, the Alameda Naval Air Station, the approach to the east end of the Bay Bridge, and Treasure Island). Such nearby liquefaction suggests the possibility of developing porewater pressures due to unrealized liquefaction in the natural (Merritt) sand at the Cypress viaduct and its associated effect on the foundation stiffnesses (in the Merritt sand) during the earthquake.

Collapse of the structure started from Bent 112 in the north and progressed southward to Bent 63. It should be noted that up to Bent 70 the near-surface soil is Merritt sand, but it then switches to Bay mud over the northern portion of the site. Likewise, there was an abrupt switch in foundation type from spread footings and short end bearing piles in the Merritt sand to long friction piles through the Bay mud occurring between Bents 71 and 72. This suggests that the possible differences in the lateral and vertical-rotational foundation stiffnesses between successive bents may have affected the progressive collapse mechanism (i.e., the collapse was arrested between Bents 70 and 63 after a transition from one soil and foundation type to another). Further complicating such consideration is the possible difference in the ground surface motion over the northern (Bay mud) versus the southern (Merritt sand) portions of the site.

Questions related to the nature of soil and foundation behavior at the Cypress Street viaduct are addressed in this and an accompanying paper by Norris et al. in this Record. In this paper subsurface conditions, site ground motions, the associated collapse, foundation types, soil properties, and porewater pressure buildup in the Merritt sand during the Loma Prieta earthquake are discussed. An earlier paper by Norris (*2*) provides an overview of foundation stiffness evaluation that is the basis for the assessment of the lateral and vertical-rotational stiffnesses at the Cypress Street viaduct presented in the following paper.

SUBSURFACE CONDITIONS, SITE GROUND MOTIONS, AND FOUNDATION TYPE

Figure 2 [after Seed et al. (*3*)] provides a plan view of the viaduct in relation to Oakland Outer Harbor to the west, Lake Merritt to the east, the approach to the Bay Bridge to the north, and the Alameda Naval Air Station to the south. In 1860 the Oakland shoreline was the edge of the Merritt sand deposit (*Qal*, Figure 3). Most of that part of modern-day Oakland to the west of this old shoreline is loose dumped or hydraulic sand fill placed in the late 1800s and early 1900s on top of the Bay mud (*Qm*, Figure 3). Therefore, the northern portion of the Cypress viaduct passed over what was once mud flats.

G. Norris, R. Siddharthan, and Z. Zafir, Department of Civil Engineering/258, University of Nevada, Reno, Nev. 89557. P. Gowda, 25 Poncetta Drive #118, Daly City, Calif. 94015.

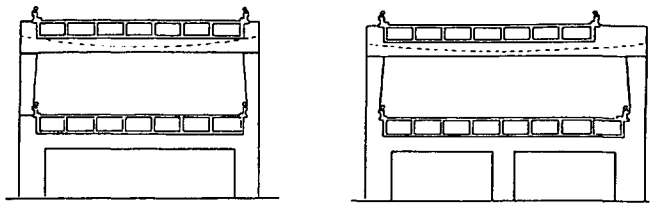

FIGURE 1 Typical two- and three-column bents at Cypress Street viaduct (*1*).

The importance of this difference in the near-surface soils in terms of possible differences in ground surface motions was amply demonstrated by the Lamont-Doherty seismological team [see, e.g., Earthquake Engineering Research Institute Report 89-03 (*4*)], who recorded aftershock motions on the Bay mud, the Merritt sand, and rock outcrop (representing bedrock motion beneath the length of the viaduct). Figure 3 compares the motion from this magnitude M4 aftershock as recorded at Stations S1, S3, and S4 and the location of these stations in relation to the viaduct and the transition from one soil type to another. Of course, the difference in amplification in going from rock (S4) to the top of Bay mud (S1) versus rock (S4) to the top of Merritt sand (S3) will not be the same (necessarily) at the higher magnitude of the Loma Prieta earthquake (M7) because of the soil's nonlinear effects.

Figure 4 shows that portion of the viaduct where the upper deck collapsed onto the lower deck. Such action progressed from Bent 112 on the northern end to Bent 63 in the Merritt sand. (Between Bents 96 and 97 the upper deck did not collapse because of the skew angle of the deck passing over 26th Street between these supports.) The collapse started at Bent 112, where the lower deck came down to the ground, and was arrested at the expansion joint between Bents 62 and 63, possibly in part because of additional lateral support to the southern section from ramps joining the upper and lower decks (and a third lower deck column and foundation) between Bents 56 and 62. However, the contribution of any change in the ground surface motion (mentioned above) and differences in the lateral and rotational stiffnesses due to an abrupt change in the soil and foundation type (on crossing over from Bay mud to Merritt sand) is probably of equal or greater importance.

Figure 5 is a profile of the near-surface soil in the vicinity of the transition from Merritt sand to Bay mud; the dots indicate pile tip elevations. It should be noted that up to Bent 35, shallow foundations were used in the Merritt sand. As shown, the Merritt sand thins out entirely between Bents 69 and 80, and pile foundations abruptly change from short end bearing piles in the Merritt sand at Bent 71 to long friction piles in Bay mud at Bent 72. This is more dramatically shown in Figure 6. [The piles are pipe piles 0.32 m (12¾ in.) outside diameter, 1 cm (⅜ in.) thick, backfilled with concrete.]

SOIL PROPERTIES AND SEISMIC POREWATER PRESSURE IN SAND

After the earthquake, the California Department of Transportation (Caltrans) undertook exploratory borings at select locations along the length of the viaduct that included two

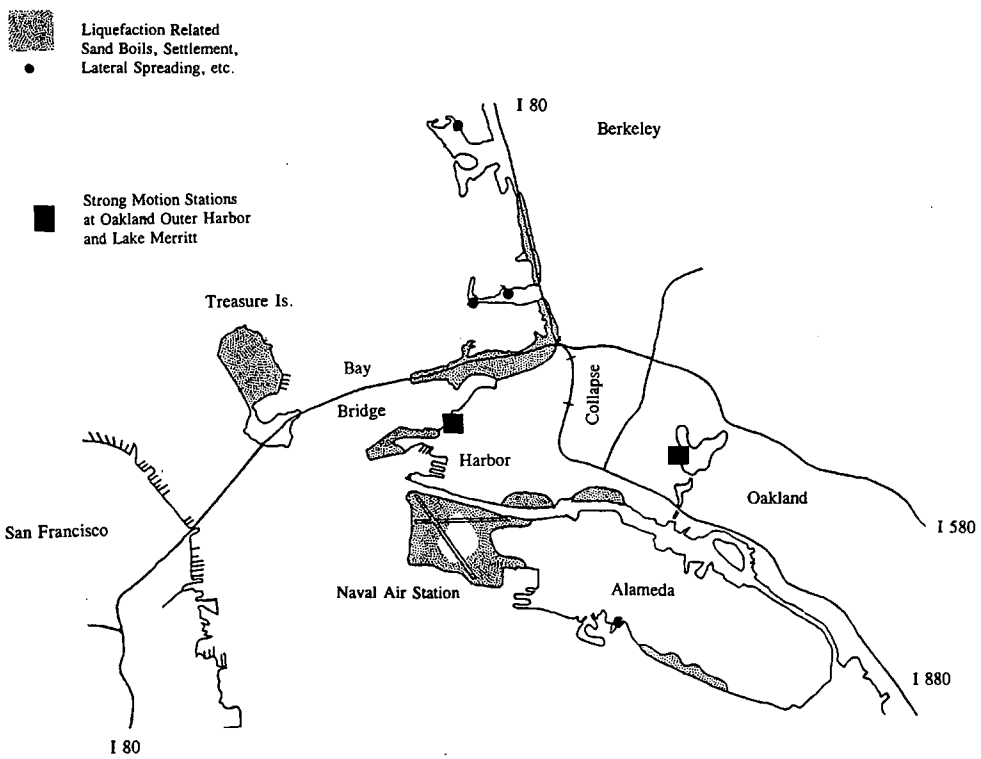

FIGURE 2 Cypress Street viaduct in relation to nearby areas of liquefaction (*3*).

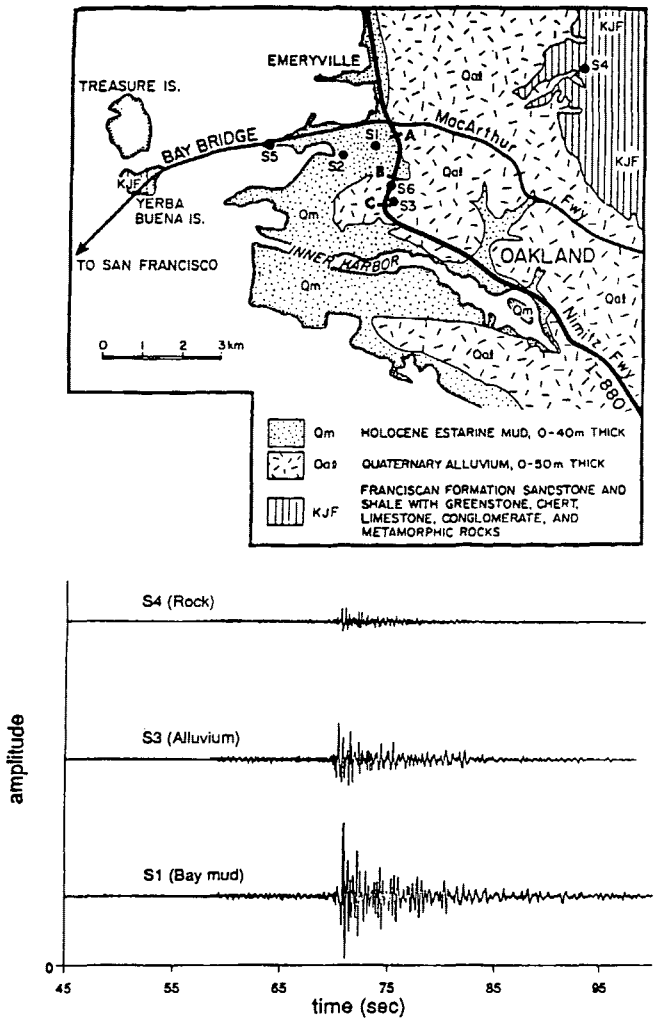

FIGURE 3 Lamont-Doherty aftershock accelerometer stations and records on Merritt sand, Bay mud, and rock (*4*).

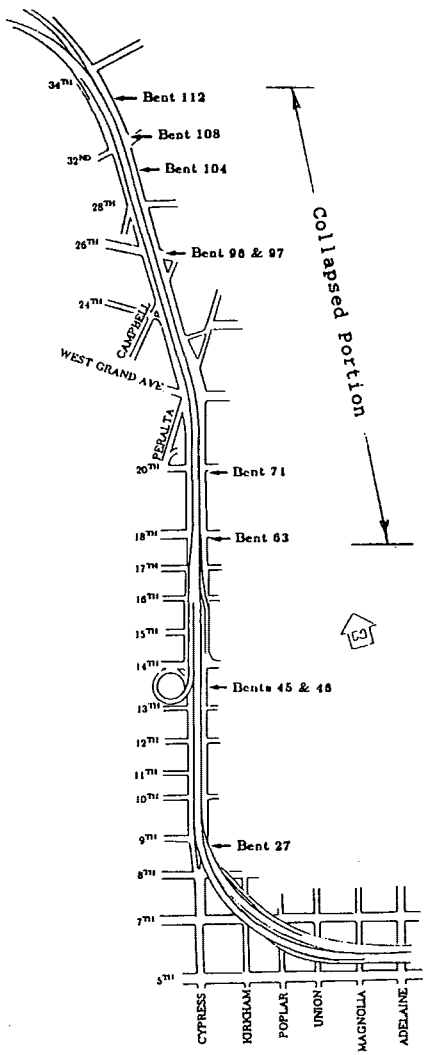

FIGURE 4 Plan view of Cypress Street viaduct showing collapsed portion (*1*).

deep holes to Franciscan greywacke at 150 m (500+ ft) depth. Figures 7 and 8 are the shallow depth logs at Bents 61 (in Merritt sand) and 97 (Bay mud) corresponding to the location of the Caltrans lateral pile group load tests undertaken subsequent to the demolition of the superstructure. The Merritt sand is a Wisconsin-age aeolian sand, and the Bay mud referred to here at the Cypress Street viaduct is actually a shallow estuarine deposit composed of intertongues of Young Bay mud, Temescal formation alluvium, and Yerba Buena mud (*5*).

Figure 9 is a characterization of the variation in vertical effective stress σ'_{vo} with depth at Bent 61, along with an estimated relative density D_r profile as established from the given Standard Penetration Test blowcounts (N) and an available correlation (*6*). A pile cap and a short end bearing pile are shown to the side for reference. Figure 10, on the other hand, is the estimated undrained shear strength variation for the Bay mud at Bent 97 established using Terzaghi's suggested correlation with blowcount, S_u (kPa) = 100 N (blows per 0.3 m)/15; that is, S_u (kips/ft^2) = N (blows per ft)/7.5. Such undrained strength values are in reasonable agreement with the few undrained strengths given on the log established from pocket penetrometer readings.

Although there were possible differences in ground surface acceleration at the top of the Merritt sand versus the Bay mud at the Cypress Street viaduct (as demonstrated in Figure 3 from aftershock response), there were no records at the site during the Loma Prieta earthquake. The nearest permanent strong-motion recording stations yielding records during the earthquake were in a two-story structure at Lake Merritt and at Oakland Outer Harbor (see Figure 2). Free-field surface records at these locations are shown in Figure 11. Although the Lake Merritt station is in Merritt sand and the Oakland Outer Harbor is in loose sand fill over Bay mud, these records are quite similar; they are slightly out of phase because of the (wave) travel time between them. The Oakland Outer Harbor peak acceleration was 0.29 g, whereas that of the Lake Merritt record was 0.26 g. Applying weighting techniques after Seed et al. (*7*), these motions yield approximately four equivalent cycles N_{eq} of a uniform amplitude of basically 0.2 g acceleration (0.65 of the peak acceleration). Since it is not clear that

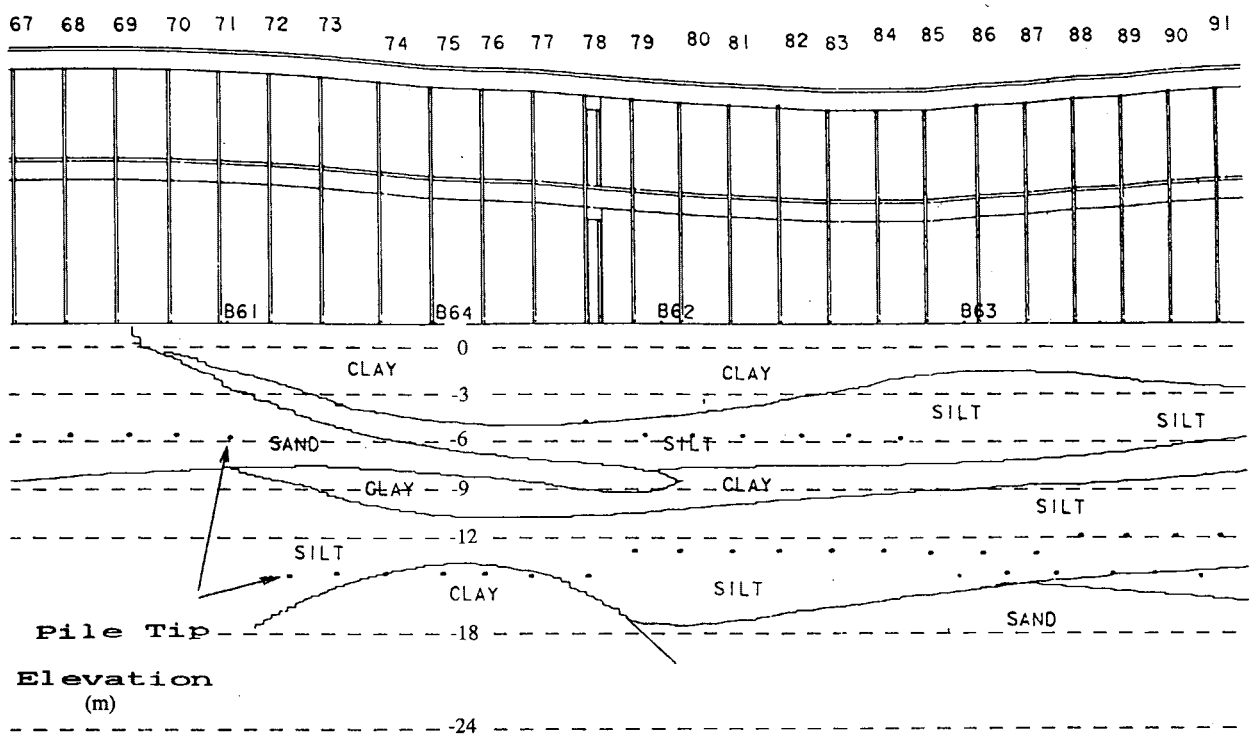

FIGURE 5 Soil conditions in transition region (*courtesy of D. Rogers*).

such motion would be representative of motions at the ground surface on the Merritt sand or the Bay mud at the Cypress Street viaduct (or if there would in fact be a difference at this higher-magnitude event), it was decided to use the given uniform equivalent motion as representative of the top of the Merritt sand to assess the possible buildup of porewater pressure causing a reduced effective stress as compared with the initial σ'_{vo} variation shown in Figure 9.

Figure 9 shows the bulb of excess porewater pressure (u_{xs}) and the reduced vertical effective stress that develops by the end of strong shaking (N_{eq} = four cycles) within the depth of the short end bearing piles at Bent 61, which would in turn affect the vertical load-carrying capacity of the piles and hence their axial stiffness. (The shaft capacity of a pile is a function of the area under the vertical effective stress diagram, whereas point capacity is related to the vertical effective stress at the pile tip.)

The means by which such u_{xs} is assessed is shown schematically in Figure 12. If at a given depth one compares the stress ratio induced by the earthquake (*8*) to the curve for the given material representing the stress ratio to cause liq-

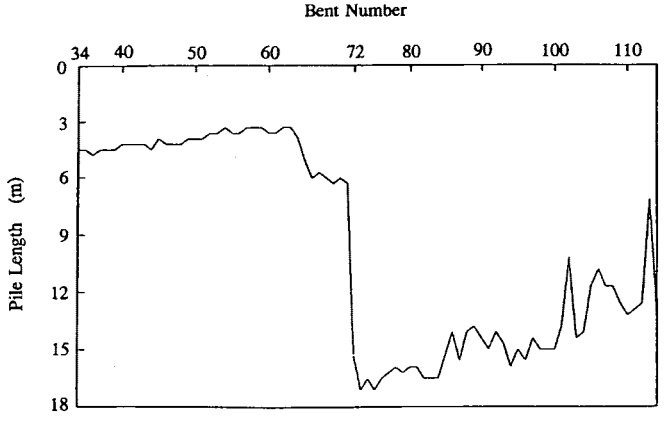

FIGURE 6 Pile length by bent location (*1*).

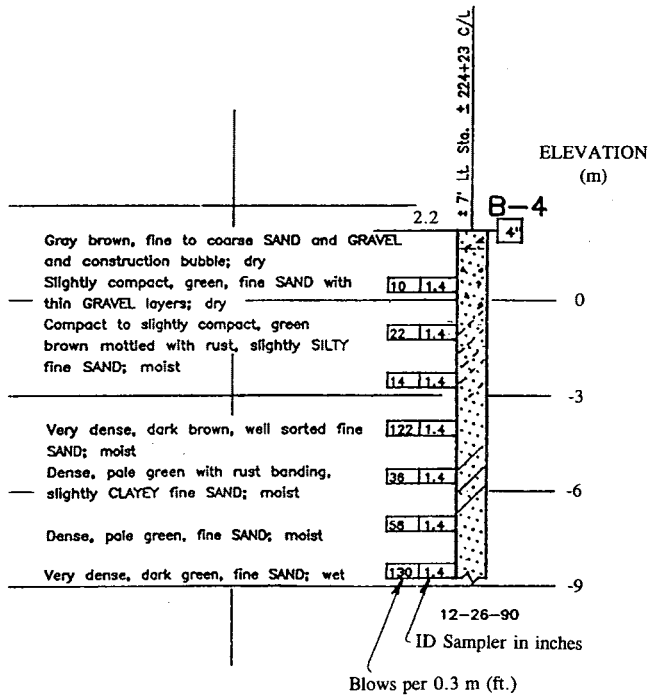

FIGURE 7 Boring log at Bent 61 in Merritt sand (*courtesy of Caltrans*).

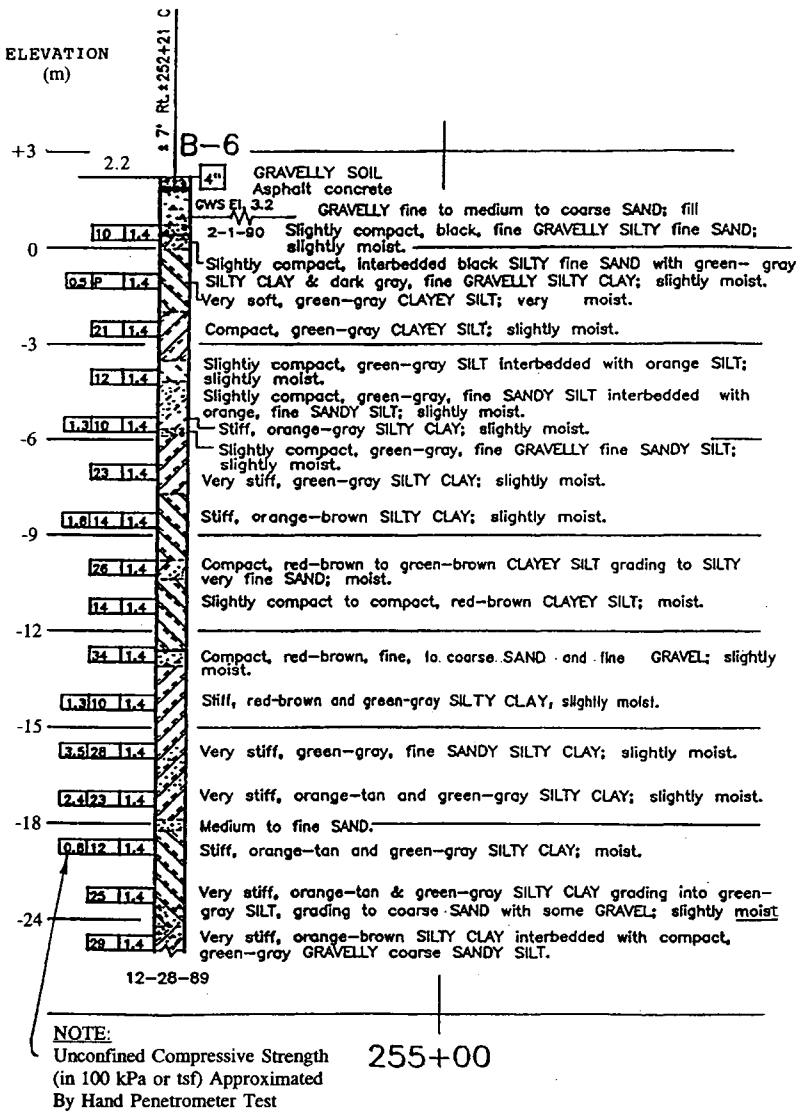

FIGURE 8 Boring log at Bent 97 in Bay mud (*courtesy of Caltrans*).

uefaction R_{liq}, and R_{eq} at its (uniform) equivalent number of cycles ($N_{eq} = 4$) is less (vertically) than R_{liq}, then there will be no liquefaction (see Figure 12a):

$$R_{eq} = 0.65(\sigma_{vo}/\sigma'_{vo})(a_{max}/g)r_d \quad (1)$$

where

σ_{vo}, σ'_{vo} = total and (original) effective stresses at the depth of interest,
$0.65a_{max}/g$ = uniform equivalent acceleration as a fraction of gravity, and
r_d = correction factor for deformable (soil) versus rigid body behavior.

However, there will still be porewater pressure buildup equal to

$$u_{xs} = r_u\sigma'_{vo} \quad (2)$$

and a reduced vertical effective stress

$$\sigma'_v = \sigma'_{vo} - u_{xs}$$

or

$$\sigma'_v = \sigma'_{vo}(1 - r_u) \quad (3)$$

where the pore pressure ratio r_u is given in Figure 12b [after Seed et al. (*8*)] as a function of the ratio N_{eq}/N_{liq}. N_{liq} is the number of equivalent uniform cycles to cause liquefaction at the stress ratio of the earthquake ($R_{liq} = R_{eq}$) as shown by the horizontal line in Figure 12a. The liquefaction curve of Figure 12a should represent the corrected blowcount N_1 and percentage fines of the sand at the depth in question. Figure 13 gives curves for different blowcounts N_1 and percentage fines as obtained from cross-plotting the Seed et al. (*8*) curves (converting magnitude M into equivalent number of cycles)

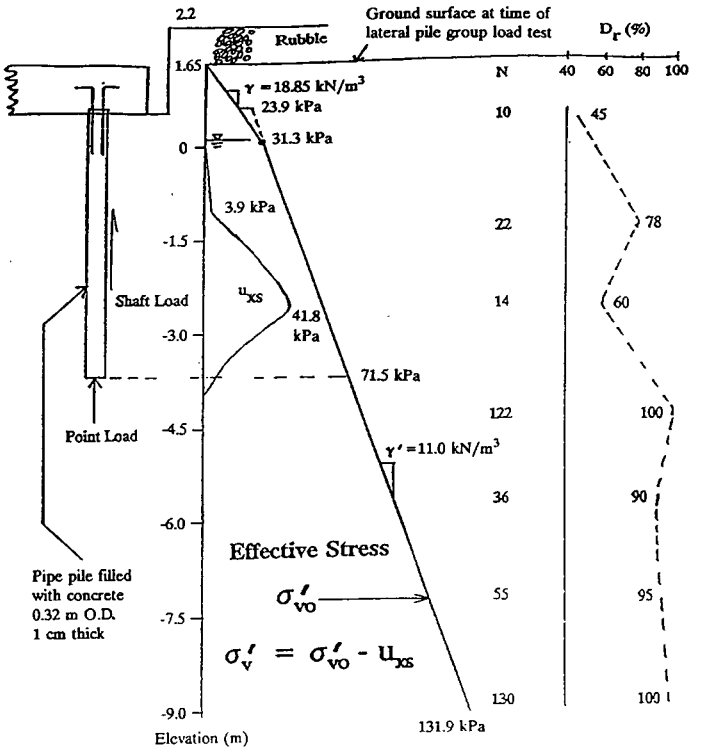

FIGURE 9 Vertical effective stress and relative density profiles at Bent 61 with the short end bearing pile shown for reference. Note: For purposes of later comparison, the ground surface, the water table, and hence σ'_{vo} shown here reflect conditions at the time of Caltrans lateral pile group tests, and u_{xs} and σ'_v reflect Loma Prieta motions (N_{eq} = 4) relative to these conditions. At the time of the earthquake, there was an added 2 to 3 ft of cover over the pile cap and the water table location may have been different.

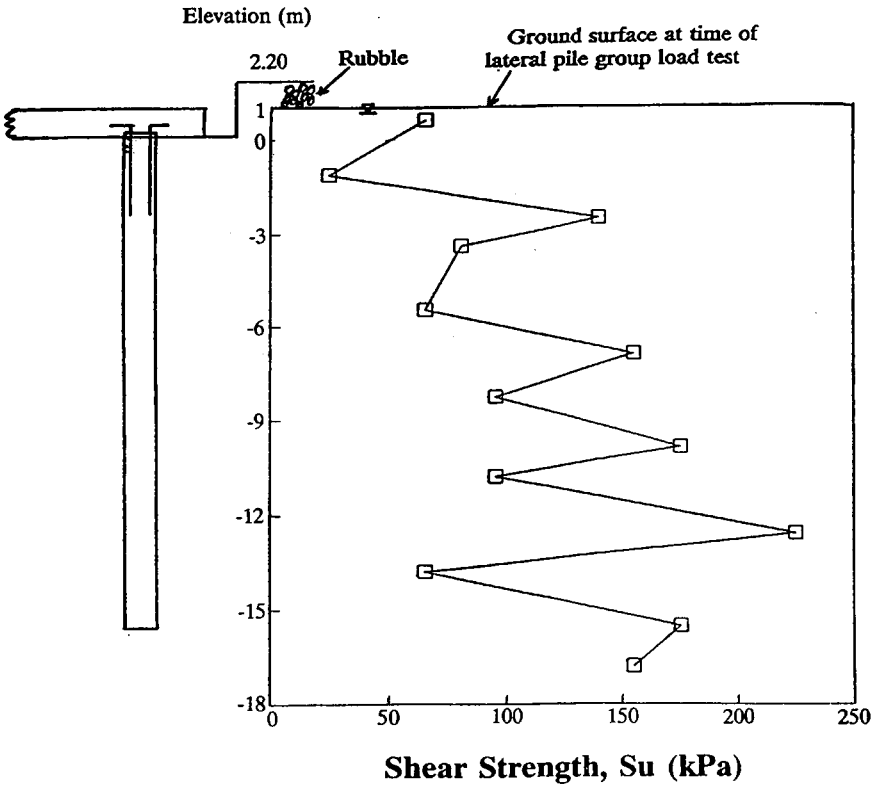

FIGURE 10 Undrained shear strength S_u profile at Bent 97.

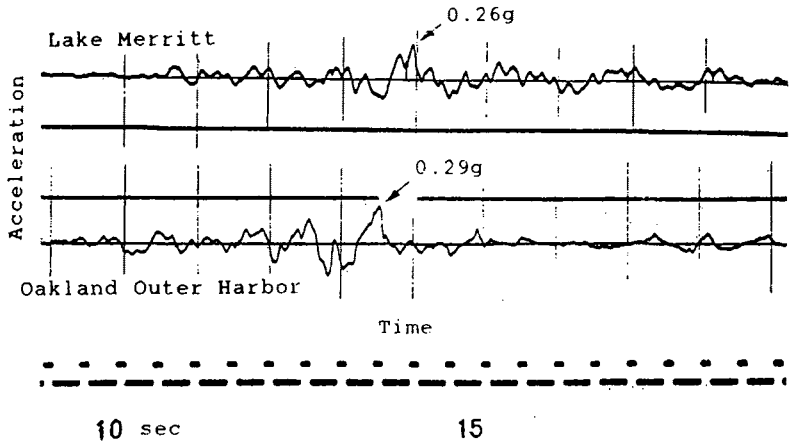

FIGURE 11 Strong shaking portion of California Strong Motion Instrumentation Program (CSMIP) free-field records at Oakland Outer Harbor and Lake Merritt.

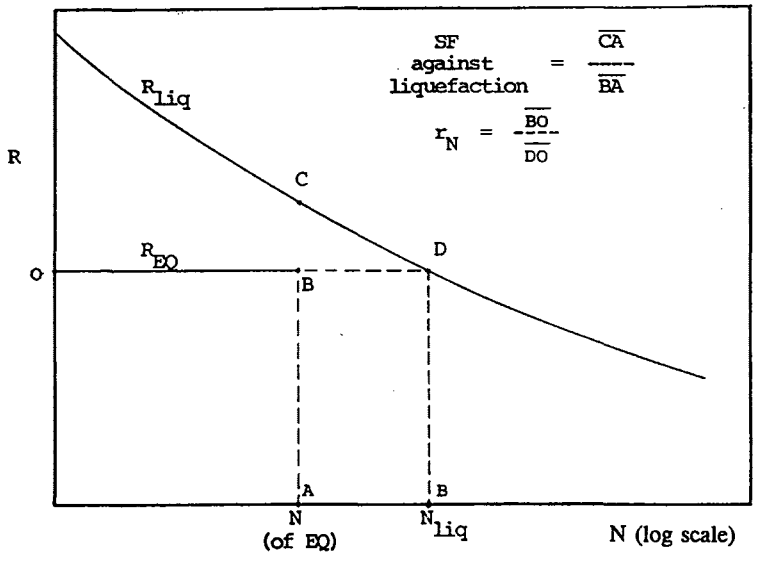

a)

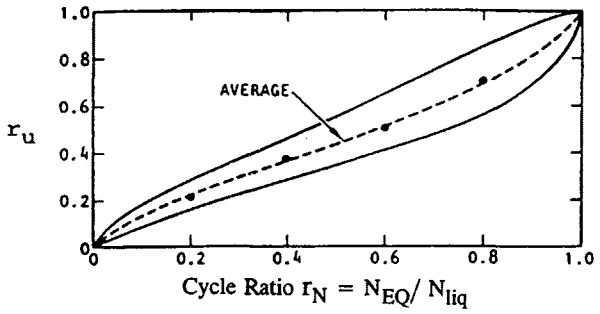

b)

FIGURE 12 Liquefaction curve (*a*) showing earthquake-induced stress ratio versus stress ratio to cause liquefaction and number of cycles to liquefaction at the earthquake-induced stress ratio and (*b*) pore pressure coefficient versus cycle ratio.

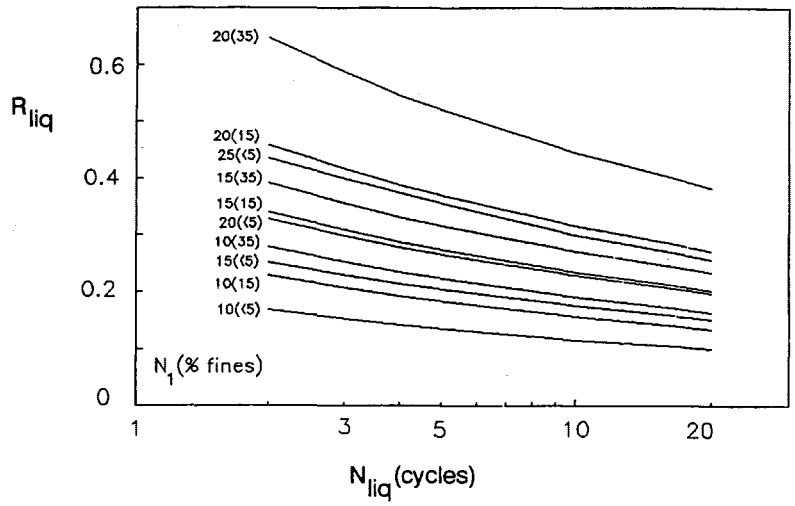

FIGURE 13 Liquefaction curves for different corrected blowcount and percent fines.

and applying a correction factor for the percentage fines (15 and >35 percent) as derived from the work of Seed et al. (*9*). The u_{xs} bulb shown in Figure 11 is the variation with depth taking the sand to be clean (<5 percent fines).

As should be noted, even though there was no liquefaction at the site, there was porewater pressure buildup in the zones of lower relative density below the water table, which by the end of strong shaking would have caused a reduced pile capacity as reflected by the reduced area of the vertical effective stress diagram. Such reduced capacity, as well as the corresponding reduced vertical pile stiffness, will be evaluated in the following paper in this Record. Although the pore pressure bulb shown in Figure 9 is for four cycles corresponding to the end of strong shaking, similar bulbs might be assessed at fewer cycles corresponding to earlier times in the record. Such time-dependent development of excess porewater pressure and the associated time-affected pile capacity and reduced pile stiffness have been demonstrated for the Meloland Overcrossing in the 1979 Imperial Valley earthquake (*10*, *11*), where (assessed) liquefaction occurred in up to three different layers at different times in the record. Here, where liquefaction did not occur, it will suffice for purposes of discussion to consider only the response at the end of strong shaking.

It should be noted that developing porewater pressures might also affect the lateral stiffness of the piles. However, laterally loaded piles develop resistance from the soil near the pile top, and from Figure 9 it would appear that the u_{xs} pressure bulb (or the majority of it) falls just below this zone of soil support. Therefore, the evaluation of lateral stiffness at Bent 61 in the following paper will be made corresponding to the effective stress profile reflected by the σ'_{vo} variation of Figure 9. Likewise, there would have been no effect on the axial and lateral stiffness of the piles in the Bay mud for these few equivalent cycles of shaking. Luckily, the duration of the Loma Prieta earthquake was much shorter than the normal M7 earthquake where an N_{eq} = 12 cycles is more typical.

SUMMARY

Subsurface conditions, site ground motions and the associated superstructure collapse, foundation types, soil properties, and porewater pressure buildup in the Merritt sand (during the Loma Prieta earthquake) at the Cypress Street viaduct have been discussed. In the following paper, methods for assessing the lateral and vertical-rotational stiffnesses [methods reviewed by Norris (*2*)] are applied to assess stiffnesses of the pile foundations at Bents 61 and 97.

ACKNOWLEDGMENT

The funding for this study was provided by the U.S. Department of Energy as part of a larger study on pile foundation stiffnesses for the seismic modeling of railroad and highway bridges. Such support is gratefully acknowledged.

REFERENCES

1. Nims, D. K., E. I. Miranda, I. D. Aiken, A. S. Whitaker, and V. V. Bertero. *Collapse of the Cypress Street Viaduct as a Result of the Loma Prieta Earthquake.* Report UCB/EERC 89-16. Earthquake Engineering Research Center, University of California, Berkeley, 1989.
2. Norris, G. M. Overview of Evaluation of Pile Foundation Stiffnesses for Seismic Analysis of Highway Bridges. In *Transportation Research Record 1336*, TRB, National Research Council, Washington, D.C., 1992, pp. 31–42.
3. Seed, R. B., S. E. Dickerson, M. E. Riemer, J. D. Bray, N. Sitar, J. K. Mitchell, I. M. Idriss, R. E. Kayen, A. Kropp, L. F. Harder, and M. S. Power. *Preliminary Report on the Geotechnical Aspects of the October 17, 1989 Loma Prieta Earthquake.* Report UCB/EERC 90-15. Earthquake Engineering Research Center, University of California, Berkeley, 1990.
4. *Loma Prieta Earthquake, October 17, 1989: Preliminary Reconnaissance Report.* EERI Report 89-03. Earthquake Engineering Research Institute, El Cerrito, Calif., 1989.

5. Rogers, J. D. Site Stratigraphy and Its Effects on Soil Amplification in the Greater Oakland Area During the October 17, 1989 Loma Prieta Earthquake. In *Proceedings of the Second International Conference on Recent Advances in Geotechnical Engineering and Soil Dynamics,* St. Louis, 1991.
6. *Design Manual: Soil Mechanics*. NAVFAC DM-7.1. U.S. Government Printing Office, Washington, D.C., 1982, pp. 14, 88, 149.
7. Seed, H. B., I. M. Idriss, F. Makdisi, and N. Banerjee. *Representation of Irregular Stress Time Histories by Equivalent Uniform Stress Series in Liquefaction Analyses*. Report EERC 75-29. Earthquake Engineering Research Center, University of California, Berkeley, 1975.
8. Seed, H. B., I. M. Idriss, and I. Arango. Evaluation of Liquefaction Potential Using Field Performance Data. *Journal of the Geotechnical Division*, ASCE, Vol. 109, No. 3, March, 1983, pp. 458–482.
9. Seed, H. B., K. Tokimatsu, L. F. Harder, and R. M. Chung. *The Influence of SPT Procedures in Soil Liquefaction Resistance Evaluations*. Report UCB/EERC-84/15. Earthquake Engineering Research Center, University of California, Berkeley, 1984.
10. Norris, G. M. Nonstable Rotational Stiffness of a Pile Group. In *Proceedings of the Third U.S. National Conference on Earthquake Engineering*, Earthquake Engineering Research Institute, Vol. 1, 1986, pp. 635–646.
11. Norris, G. M. A Seismic Analysis: Meloland Overcrossing During the 1979 Earthquake. In *Geotechnical Special Publication 17: Centrifugal Models and Field Performance*, ASCE, 1988, pp. 88–117.

Publication of this paper sponsored by Committee on Foundations of Bridges and Other Structures.